Surface and Photochemistry

(BL2B1, 3A1, 4A1, 4A2, 5B, 6B, 8A)

(BL4A2)

SR etching of SiO_2 using a contact cobalt mask

C.Wang[1], Z.Wang[2], S.More[1], Y.Nonogaki[1], S.Yamamura[2], S.Fujiki[2], M.Takizawa[2], T.Urisu[1, 2]
[1]*Institute for Molecular Science,* [2]*The Graduate Univ. for Advanced Studies*

We have studied a new etching technique, which can be applied to the area selective deposition of SAM and biomaterial on silicon wafers. We use SF_6+O_2 as the reacting gas and a cobalt thin film as the contact mask. The cobalt mask was found to show strong resistibility for SR, while it can be easily removed with dilute acid. The roughness of the surface after the SR etching was sufficiently small to fabricate an well-ordered SAM on silicon wafers.

The silicon dioxide film (~ 205 nm) was thermally grown on n-type (80-120 ohm · cm) Si (100) wafer. A cobalt thin film (~ 200 nm), which was fabricated on the silicon oxide surface by using a sputtering technique was used as the contact mask. The gas pressure for O_2 and SF_6 was 0.05 torr and 0.002 torr, respectively. The beam current was about 200 mA. The irradiation dose of SR beam was about 2000 mA · min.

The depth profile (Fig. 1) of the etched pattern indicates that SR irradiation with flowing SF_6 and O_2 can effectively etch the silicon dioxide and completely stop on the silicon surface. The cobalt mask shows strong resistibility for SR etching. Furthermore, the cobalt was found to be easily removed by diluted HNO_3 or HF solution. Consequently, the cobalt can be used as a good mask for SR etching

The cross section of the etched pattern was observed with scanning electron microscopy (SEM). Due to the good directivity and short wavelength nature of synchrotron radiation beam, the SR etching for SiO_2 is anisotropic, and the sidewall of the etching pattern is very steeper. The AFM topography (Fig. 2) shows that the roughness of the surface after SR was about 1 nm. These flat surfaces are fit for depositing well-ordered SAM and biomaterials.

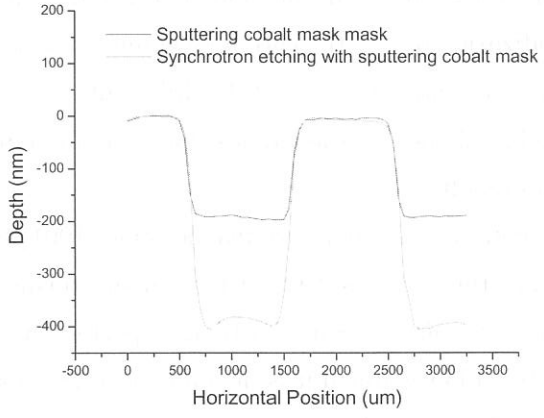

Fig. 1

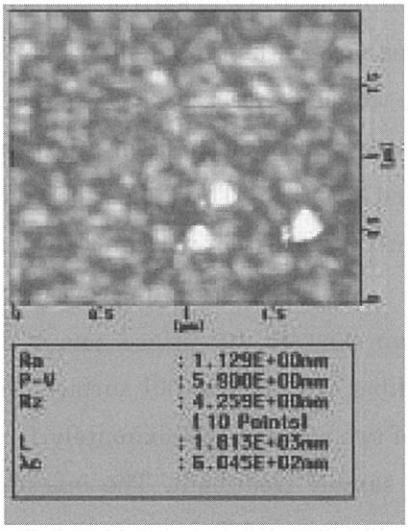

Fig. 2

(2B1)

Ion desorption from the $SrTiO_3(100)$ surface

S. Tanaka[1], K. Mase[2], and S. Nagaoka[3]

[1]*Department of Physics, Graduate School of Science, Nagoya University, Furo-cho, Chikusa, Nagoya 464-8602, Japan*

[2]*Institute of Material Structure Science, Tsukuba 305-0801, Japan*

[3]*Chemistry Group, Department of Fundamental Material Science, Faculty of Science, Ehime University, Matsuyama 790-8577, Japan*

Desorption induced by electronic transition (DIET) from solid surfaces has been studied extensively in recent decades, and a general mechanism of the ion desorption induced by core-level excitation was proposed by Knotek and Feibelman. It is based on the results they obtained when measuring the electron stimulated desorption (ESD) yield of O^+ from TiO_2, whose desorption threshold correlates with the Ti3p core excitation threshold but not with the O2s or the valence excitation. In the Knotek-Feibelman (KF) mechanism, a Ti3p core hole is produced by a primary excitation and decays by means of an *inter*atomic Auger process because there are no higher-lying occupied electronic states except for the O2s and O2p orbitals. (i.e., it is the "maximal valency" state). If two Auger electrons and an additional electron (due to, for instance, double Auger decay) are emitted by the oxygen atom, the remaining O^+ ion desorbs as a result of the Coulomb repulsion from the surrounding Ti^{4+} ions.

Recently, we have proposed another mechanism based on the investigation on the $TiO_2(110)$ and the ZnO(1010) surfaces by means of the electron-ion coincidence (EICO) spectroscopy. In the proposed mechanism, the creation and desorption of O^+ are driven by a charge transfer through the O2p-Ti3d hybridization due to the core hole potential at Ti (the Kotani-Toyozawa mechanism). TiO_2 has an unoccupied 3d orbital while ZnO has fully occupied 3d orbital. Thus, the proposed model predicts that the ion desorption occurs only on TiO_2, and is consistent with our experimental result.

$SrTiO_3$ is a typical perovskite-type metal oxide. There are two possible (100) planes that can exist on its surface; one is SrO, and the other is TiO_2. After ion-sputtering and annealing, the $SrTiO_3(100)$ surface contains both planes. Some authors reported that the ratio of two areas is approximately 1:1, but the other claimed it is dependent on the history of the sample treatment. The investigation of the ion desorption from this surface is of interesting because Ti is transition metal and Sr is not. Therefore, if one assumes a simple

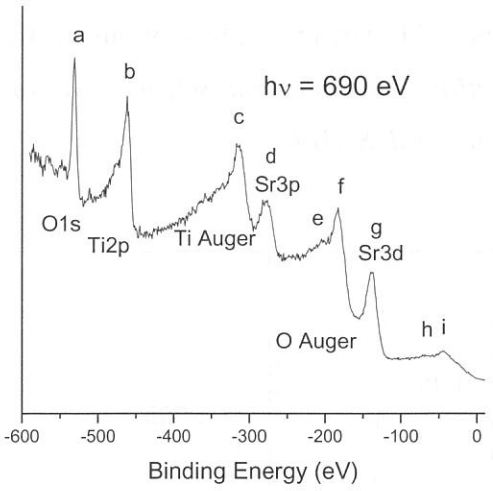

Figure 1

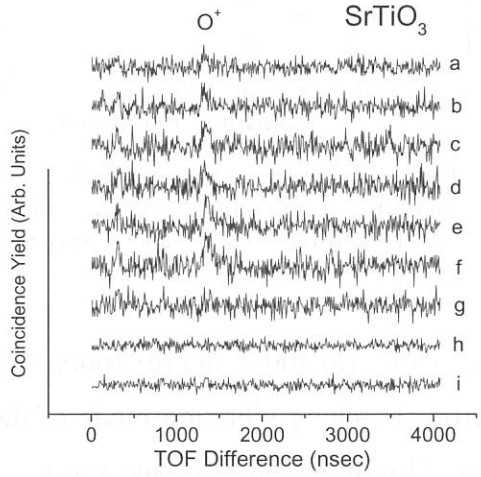

Figure 2

electronic configuration in which the bonding between Ti and O and that between Sr and O in $SrTiO_3$ are the same as those respectively in SrO and TiO_2, it is expected that the ion desorption occurs only on the excitation of the Ti-core level.

All the experiments were carried out at BL2B1 of UVSOR. The $SrTiO_3$(100) surface was Ar^+-sputtered and annealed in the vacuum and oxygen ($1x10^{-6}$ Torr) to obtain the stoichiometric surface with small number of oxygen vacancy. The ratio of SrO and TiO_2 domains is not known. Figure 1 shows the photoelectron spectrum of the taken at hν=690eV. Several peaks are observed, and indicated as a – i. These are photoelectron from the core-level and Auger electron emissions, as shown in the figure. Figure 2 shows EICO spectra of using the photoelectrons of a – i in Fig.1. O^+ desorption is observed for the curves of a – f, which are the photoelectron emission from the O-core (a), and Ti-core (b) levels, and Auger electron emission of O-core (e,f), and Ti-core (c,d) levels. Note that the peak d in Fig. 1 is also contributed from the Sr-core electron emission. Meanwhile, no peak is observed in the coincidence spectrum g, which indicates that the excitation of the Sr3d electron does not efficiently yield the ion desorption. This result is consistent with our proposal on the desorption mechanism, and contradict against the KF model, because the maximal valency condition is satisfied in SrO as well as TiO_2. However, according to the experimental results using a different photon energy, the the desorption induced by the Sr 3p and 3d electron excitation is clearly observed, even though their efficiencies are smaller than the Ti and O core-electron excitation. More work, including a quantitative comparison of ion desorption probabilities among the core-levels, is needed and in progress.

(BL4A2)

Reactivity of the Nearly Ideally H-terminated Si(100)-2×1 Surface with Water

Z.-H.Wang[1], H.Wanatabe[3], S. Nanbu[2], J. Maki[2], M. Aoyagi [1,2] , K. Ooi[3] and T. Urisu[2]

The Graduate Univ. for Advanced Studies[1] / Institute for Molecular Science[2], Nation. Insti. Advanc.Indust. Sci. Technol. Shikoku[3]

The ideally H-terminated Si(100) surface is very important from both viewpoints of surface science and semiconductor process technology. Surprisingly the detailed investigations are very few since the experimental difficulties on detection of surface species on one hand and theoretical expensive on the other hand. In this work, the BML-IRRAS technique was used to monitor the water reaction with ideally H-terminated Si(100)-2×1 surface for the first time. In Fig. 1, IR spectra of nearly ideally H-terminated Si(100) 2×1 surface (a), and the changes of the IR spectra by exposing the surface (a) to (b) 50L, (c) 200 L and (d) 1000L water vapor. The 2100 cm^{-1} peak is assigned to the symmetric stretching vibration mode of the coupled monohydride. From Fig. 1, it is clear that the H-termination has passivation effects for dissociative adsorption of water. But, it is also clear that the surface is still highly reactive with water and easily oxidized. The complex peak assignment is now under investigation combined with an ab initio molecular orbital (MO) calculation of the cluster model. The initial oxidation mechanism of water with H-terminated Si(100)-2×1 surface is also proposed.

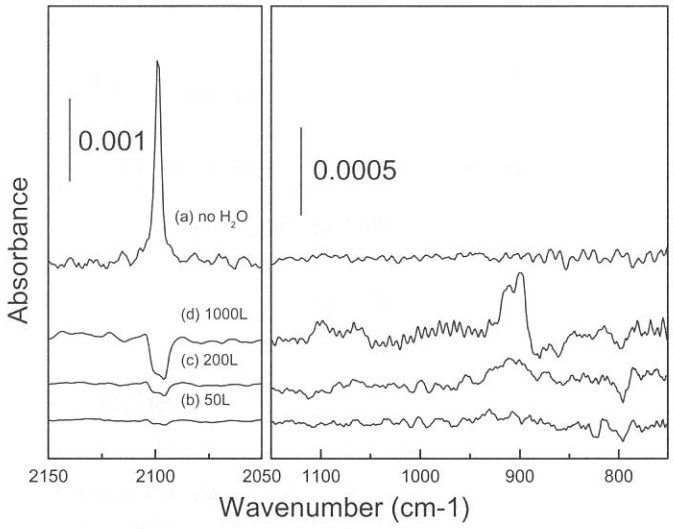

Fig. 1 IR spectra of (a) nearly ideally H-terminated Si(100)-2×1 and (b), (c), (d) after the 50, 200 and 1000L exposure to water vapor, respectively.

(BL4A2)

Nearly Ideally Hydrogen Terminated Si(100) Surface and IR-spectrum Width Broadening Due to Hydrogen Diffusion into the Subsurface

Z.-H. Wang[2], N. Yabumoto[3], T. Urisu [1,2] Wang@ims.ac.jp,

The Graduated Univ. for Advanced Studies[1] / Institute for Molecular Science[2], NTT Advanced Technology Corporation[3]

Nearly ideally H-terminated condition for Si(100)-2 × 1 surface is determined from the dependence of the peak intensity and the linewidth of the coupled monohydride symmetric stretching vibration on the hydrogen exposure and the exposure temperature, which has been investigated with infrared reflection absorption spectroscopy (IRRAS) using $CoSi_2$ buried metal layer substrate. It was found that even for nearly ideally H-terminated surfaces, the linewidth significantly changes depending on the hydrogen exposure and the exposure temperature. At low temperature region (<600K), the line width broadening was explained by the inhomogeneous of surface caused by dihydride species SiH_2 existence. At higher temperature region (>700K), the line width broadening was explained by the decomposition of coupled monohydride and background water adsorption contamination. In the region of (600K ~ 700K), the line width broadening can not simply explained by these effects since no dihydride species can be detected and no water contamination trace exist. The concentration of deuterium atoms incorporated in the Si bulk is measured by temperature programmed desorption. It is proportion with the line width. From these experimental facts it is concluded that hydrogen diffusion into the subsurface of Si has a significant influence on the linewidth broadening.

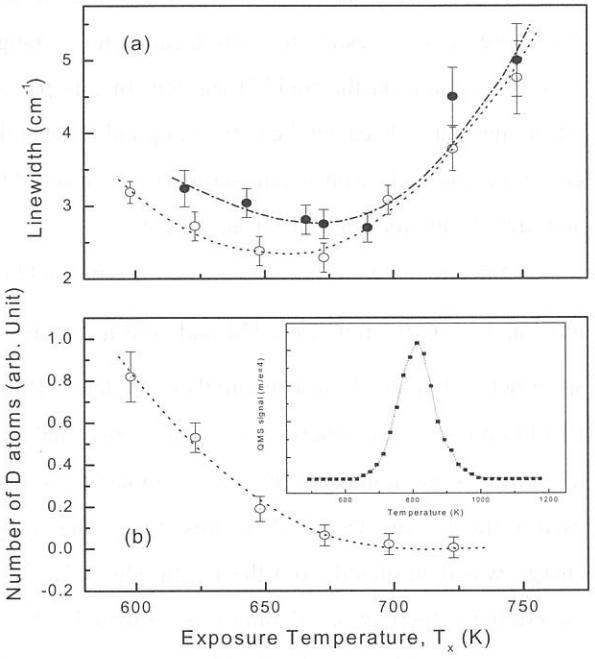

Fig. 1 Dependence of linewidth and desorption of D atoms incorporated into the bulk on the exposure temperature.

(BL5A)

Local atomic arrangement of Si(111)√3x√3-(Pb,Sn) surface

J. Yuhara, T. Takada, D. Nakamura†, K. Soda, M. Kamada*

Graduate School of Engineering, *Nagoya University, Nagoya, 464-8603, Japan*
*UVSOR, Institute for Molecular Science, Myodaiji, Okazaki 444-8585, Japan**

Recently, great attention has been focused on the understanding of atomic arrangement and electronic structure of binary adsorbates on the semiconductor surface to control crystalline growth mode, such as perfect flat interface and nano-dots. In the case of (Pb,Sn) binary adsorbates on the Si(111) surface, they form unique 2√7x3 and √7x√3 structures at the total coverage of 0.7 ~ 0.8 ML, although they are immiscible in bulk. We have also observed that co-adsorbates of Pb and Sn form a √3x√3 reconstruction at the total coverage of 1/3 ML. Therefore, it is interesting to study local atomic arrangements and electronic structures of (Pb,Sn) co-adsorbates at low coverage on the Si(111) surface. In this paper, the Si(111)√3x√3-(Pb,Sn) surface at single and binary adsorbates have been studied by topographic scanning tunneling microscopy (STM) and Pb 5*d* and Sn 4*d* core-level photoelectron spectroscopy (PES) in order to discriminate the adsorbate elements on the STM images and identify the local atomic arrangement.

Specimens were mirror-polished n-type Si(111) wafers with a resistivity of 3 Ω cm in sizes of 15x3x0.5 mm^3 and 15x6x0.5mm^3 for STM and core-level PES measurements, respectively. In the PES measurement, the specimen was placed on a manipulator under $5x10^{-9}$ Pa base pressure in the UHV chamber equipped with a LEED optics, a hemispherical electron energy analyzer ($\Delta E = 0.04$ eV) with an angular acceptance of ± 8° at the normal emission angle, and two evaporation sources for Pb and Sn. Excitation photon energy of 52 eV was used at the 45° incident angle in this study. The energy spread of excitation photon was 0.04 eV. The binding energy was determined from the Fermi edge of a Ta plate that holds the Si wafer. The total energy resolution including the thermal broadening was estimated to be about 0.10 eV from the Ta Fermi edge.

Typical topographic STM images of the Si(111)√3x√3-(Pb,Sn) surface are shown in Fig.1 (a) for the filled states and (b) for the empty states. Observed spots in the STM images can be classified into three type of spots; white and gray (α), gray and white (β), and black and gray (γ), in the filled- and empty-state images, respectively. The Pb 5*d* and Sn 4*d* core-level photoelectron spectra were measured for mosaic √3x√3-Pb, √3x√3-Pb, √3x√3-(Pb,Sn), √3x√3-Sn, and mosaic √3x√3-Sn surfaces to investigate the chemical states of Pb and Sn adsorbates. Typical core-level PES spectra are shown in Fig.2. As is seen in Fig.2 (b) and (d), the √3x√3-Pb and √3x√3-Sn surfaces show two major surface chemical shifted components in the Pb 5*d* and Sn 4*d* core-level spectra, respectively. This is ascribable to charge density wave or dynamical fluctuation of Sn adatoms between two different vertical positions above T4 site [1], which are detectable on PES but not in STM because of the z scale resolution limit and the difference in the probing time scale [2,3]. The peak positions and shape of Pb 5*d* and Sn 4*d* core-levels of the √3x√3-(Pb,Sn) surface are similar to those of the √3x√3-Pb and √3x√3-Sn surfaces. This suggests that there is no specific charge transfer between Pb and Sn at the √3x√3-(Pb,Sn) surface and that chemical states of Pb and Sn are almost the same as those of the √3x√3-Pb and √3x√3-Sn surfaces. Since the minimum atomic distance between adsorbates in the √3x√3 reconstruction at the coverage of 1/3 ML is 0.665 nm, it may be reasonable to have no direct interaction between Pb and Sn adsorbates. On the other hand, the Pb

5*d* and Sn 4*d* core level spectra of the mosaic √3x√3-Pb and mosaic √3x√3-Sn surfaces show one major component, respectively. The binding energies of Pb 5*d* and Sn 4*d* spectra of mosaic √3x√3-Pb and mosaic √3x√3-Sn surfaces are almost equal to those of lower binding energy component on the √3x√3-Pb and √3x√3-Sn surfaces, respectively. This result agrees well with the result reported previously [1,2,4]. These results indicate that Pb and Sn atoms are stabilized at certain height or in one charged state on the mosaic √3x√3 surfaces. These results also suggest that the Pb and Sn heights, or charged states, stabilized at the mosaic √3x√3 surface are similar to those at the √3x√3 surface.

From the topographic STM images including domain boundary of the 7x7 and √3x√3-Pb surfaces and that of the 7x7 and √3x√3-Sn surfaces, it is found that the averaged spot heights at Sn are 0.03~0.05 nm higher than those at Pb in the filled state image, while they are 0.05~0.07 nm lower in the empty state image. This bias dependence of the corrugation of Pb and Sn is closely related to those of the spots α and β on the √3x√3-(Pb,Sn) surface in Fig.1. Thus, we conclude that Sn and Pb are located at α and β positions, respectively. Since Si adatoms are easily replaced with Pb and Sn in √3x√3 surface and their STM images at the Si adatom position show black and gray spots in filled and empty state images, respectively [5], it is considered that Si adatoms are located at the γ position.

References

[1] J. Avila, A. Mascaraque, E. G. Michel, M. C. Asensio, G. Le Lay, J. Ortega, *et al*, Phys. Rev. Lett. 82 (1999) 442.

[2] M. Göthelid, M. Björkqvist, E. G. Michel, M. C. Asensio, G. Le Lay, C. J. Karlsson, Phys. Rev. B52 (1995) 14532.

[3] R. I. G. Uhrberg, H. M. Zhang, T. Balasubramanian, S. T. Jemander, N. Lin, and G. V. Hansson, Phys. Rev. B62 (2000) 8082.

[4] R. I. G. Uhrberg, H. M. Zhang, T. Balasubramanian, Phys. Rev. Lett. 85 (2000) 1036.

[5] J. M. G. Rodriguez, J.-Y. Veuillen, R. C. Cinti, Surf. Sci. 377/379 (1997) 45.

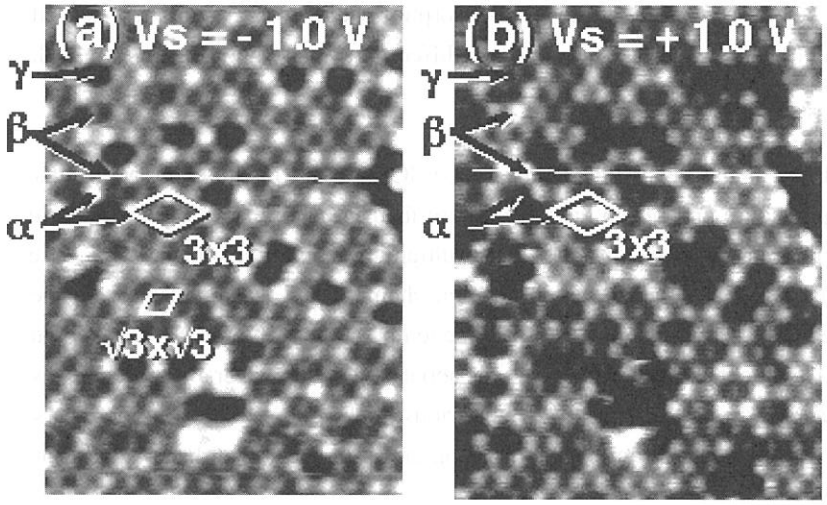

Fig.1 STM images obtained from the √3x√3-(Pb,Sn) surface at sample biases of -1.0 V (filled state) (a) and +1.0 V (empty state) (b). Spots are classified into three type of spots; white and gray (α), gray and white (β), and black and gray (γ) in the images (a) and (b), respectively. A √3x√3 unit cell is indicated in the figure as well as 3x3 unit cell.

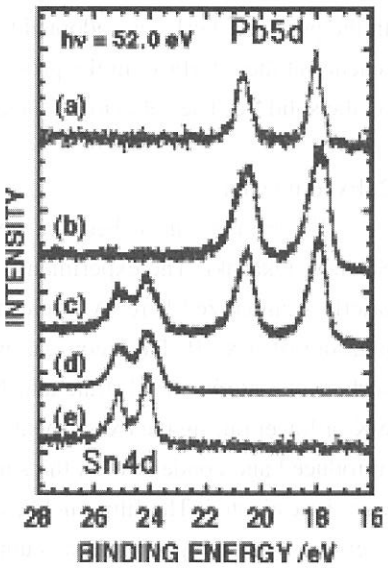

Fig.2 Pb 5*d* and Sn 4*d* photoelectron spectra of mosaic √3x√3-Pb surface with 1/6ML Pb (a), √3x√3-Pb with 1/3ML Pb (b), √3x√3-(Pb,Sn) (c), √3x√3-Sn with 1/3 ML Sn (d), and mosaic √3x√3-Sn with 1/6 ML Sn (e) after background subtraction.

(BL5B)

Measurements of Total Yields of Exciton-Induced Desorption from Argon Films Condensed on Solid Neon

Takashi Adachi, Takato Hirayama*, Ichiro Arakawa and Makoto Sakurai**

Department of Physics, Gakushuin University , Mejiro, Toshima, Tokyo 171-8588.
**Department of Physics, Rikkyo University , Nishi Ikebukuro, Toshima, Tokyo 171-0021.*
***Department of Physics, Kobe University, Rokkodai-cho, Nada-ku, Kobe 657-8501.*

1. Introduction

Electron or photon irradiation of the surface of rare gas solids produces the electronic excitations which can be followed by the desorption of various kinds of particles. Investigation of the desorption induced by electronic transitions (DIET) will reveal the dynamics of the electronic excitations and relaxations in solid and, especially, at the surface. DIET at the surface of rare gas solids has been extensively studied since 1980s [1]. We have reported the results of measurements of absolute photo-desorption yields from the surface of solid Ne [2], Ar [3, 4] and Kr [5] at excitonic excitation regime. At a film, which is thicker than 400 atomic layers, condensed on a metal substrate, the absolute photo-desorption yields are about 1.5, 0.2, and 0.03 atoms/photon for Ne, Ar, and Kr, respectively, at the excitation energy of the first order bulk exciton. The quantitative analysis of the absolute desorption yields and the thickness dependence reveal relaxation channels from the primary excitonic excitation to the desorption. The desorption yield of Ne was quantitatively explained by the internal sputtering mechanism [2]. In the case of Ar [3, 4] and Kr [5], the dominant desorption mechanism is the excimer dissociation which is followed by collision cascade.

The diffusion of excitons and these behavior at the interface between a solid rare gas and a substrate are important process to be considered for the estimation of the desorption yields and these thickness dependence. In the previous works, we adopted the assumption that the excitonic excitation is quenched immediately when it reaches at the interface. In the present study, we measured the photo-desorption yields from Ar films condensed on the solid Ne. The behavior of the exciton at the interface between two different rare gas solids are investigated.

2. Experimental

Experiments have been carried out at the beam line BL5B in UVSOR of the Institute for Molecular Science, Okazaki. The experimental procedure and set-up have been described in detail elsewhere [5] and are briefly summarized here. A liquid helium cryostat was installed in an ultrahigh-vacuum chamber with a base pressure of 5×10^{-9} Pa. Neon gas was introduced into the main vacuum chamber and was condensed on the surface of a platinum substrate attached to the liquid helium cryostat. The temperature of the sample was kept at 6 K or lower during the experiments. The thickness of the solid Ne was about 200 atomic layers. Argon gas was introduced and condensed on the surface of the solid Ne. Ar films of various thickness up to 800 atomic layers were investigated. The film thickness was calculated from the exposure on the assumption that the condensation coefficient of each gas at 6K was unity.

The absolute desorption yield was calculated from the absolute values of the intensity of the incident photons and of the number of Ar atoms desorbed. The absolute number of the incident light was monitored by measuring a photoelectron current emitted from the gold mesh which was installed in the beam line. The absolute number of the desorbed atoms was calculated from the rise of partial pressure of Ar, which was measured by a quadrupole mass spectrometer, during the irradiation of the sample and the total pumping speed for Ar.

3. Results and Discussions

The dependence of the total photo-desorption yields of Ar on the incident wavelength is shown in Fig. 1 for three different film thicknesses. For the film of 3 atomic layers in thickness, clear peaks are observed at 103 nm and 101 nm, which corresponds to the excitation energy of the first order bulk excitons, B1(3/2) and B1 (1/2), of solid Ar, respectively. For the film of 150 atomic layers, an additional peak appear at the wavelengths corresponding to the second order bulk (B2, 91 nm (3/2)) exciton. For the 520 atomic layers film, the small shoulder at 106 nm and the peak at 96 nm are observed, which corresponds to the creation of the second order surface (S2) and the first order surface (S1) excitons, respectively. The spectrum at 520 atomic layers is almost identical to that of the thick Ar film which is solely and directly condensed on the metal substrate.

Figure 2 shows the thickness dependence of the absolute desorption yields at B1 exciton excitation energy for two different systems; the Ar film condensed on the solid Ne and that on the metal substrate. The difference of the desorption yields between them at the thickness less than 10 atomic layers is originated from the difference in the behavior of the exciton at the interface. In the case of Ar on metal, the exciton is immediately quenched when it reaches at the surface of the metal substrate. In thin films, therefore, it results in low desorption yields. On the other hand, in the case of the Ar film condensed on solid Ne, the interface of Ar/Ne plays as a reflector for B1 exciton of Ar because the excitation energy of B1 exciton can not be transferred to solid Ne. Consequently the high desorption yields are observed at thin Ar film condensed on solid Ne. The quantitative analysis of the absolute desorption yields are now in progress.

References

[1] for recent review, see I. Arakawa, Molec. Crystal Liq. Crystal, **314**, 47 (1998), M. Runne and G. Zimmerer, Nucl. Instrum. Meth. Phys. Res. B **101**, 156 (1995).

[2] I. Arakawa, T. Adachi, T. Hirayama and M. Sakurai, Surf. Sci. **451**, 136 (2000).

[3] T. Adachi, T. Hirayama, I. Arakawa and M. Sakurai, UVSOR Act. Rep. 1999, UVSOR-**27**, 178 (2000).

[4] T. Adachi, T. Hirayama, I. Arakawa and M. Sakurai, UVSOR Act. Rep. 2000, UVSOR-**28**, 208 (2001).

[5] T. Adachi, T. Hirayama, I. Arakawa and M. Sakurai, in preparation.

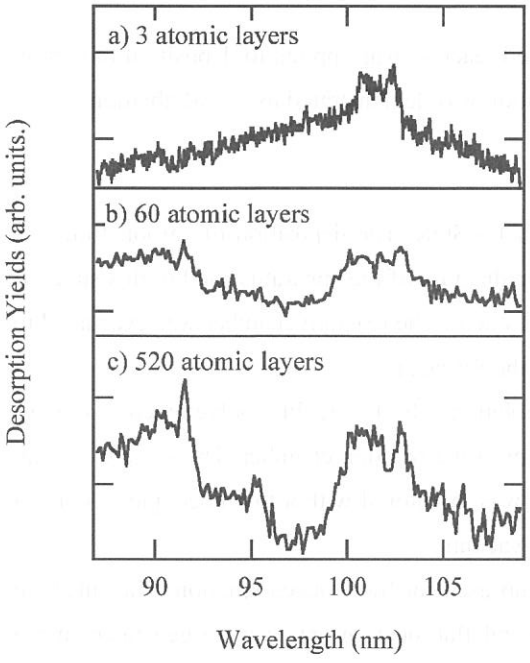

Fig. 1 Wavelength dependence of total desorption yields of Ar condensed on solid Ne.

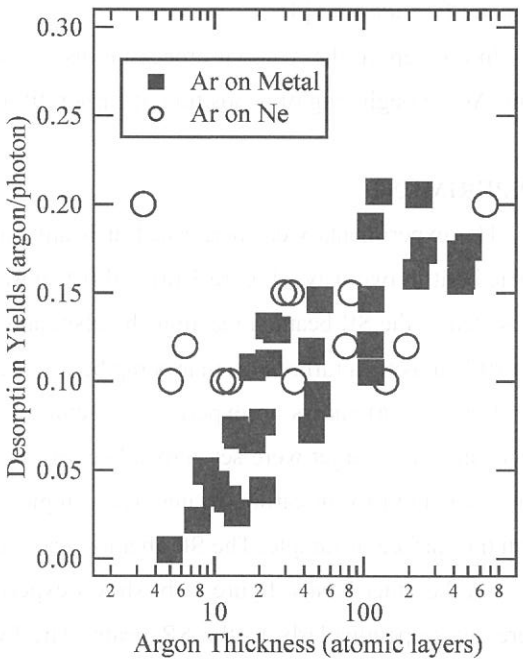

Fig. 2 Thickness dependence of absolute desorption yields at the excitation of B1 exciton.

(BL8A)

Deposition of Carbon Film Using Synchrotron Radiation Ablation

Hisao Nagai, Masaru Hori and Toshio Goto,
*Koji Katou, *Kouhei Ito and *Mineo Hiramatsu

Department of Quantum Engineering, Nagoya University,
Chikusa-ku, Nagoya, 464-8603
**Department of Electrical and Electronic Engineering, Meijo University,*
Tempaku-ku, Nagoya, 468-8502

INTRODUCTION

Electron field emission from various carbon materials has recently attracted much attention for their promising applications in displays and other microelectronic devices. Diamond, nanodiamond and diamond-like carbon are widely investigated and demonstrated to initiate emission at reasonably low fields. Among them, carbon materials such as nanodiamond and diamond-like carbon exhibit conspicuously excellent field emission characteristics, including very low threshold electrical fields, large emission current density, and high emission site density.

Previously, we demonstrated the anisotropic micromachining and film formation of Teflon (fluorocarbon polymer) using synchrotron radiation (SR) ablation process [1, 2]. Moreover, in order to clarify the mechanism of SR ablation, we have performed polytetrafluoroethylene (PTFE) micromachining by selecting the photon energy distribution of incident SR beam with carbon (C) membrane and carbon/magnesium fluoride / carbon (C / MgF_x / C) triple-layered membrane as filters. From these results, the photons with energy below 120 eV were found to contribute to the ablation of PTFE [3]. In addition, SR ablation was applied to pattern formation of metal fluoride film [4].

In this report, the material processing using the SR induced reaction was applied to deposition of carbon film. As the beginning of deposition of carbon film, the deposition was demonstrated using SR ablation.

EXPERIMENT

The experiments were performed at beam line BL-8A of UVSOR. The deposition of carbon film was carried out in two ways. Figure 1 (a) and (b) show a schematic diagram of the apparatus used in this study. It consisted of the SR beam, a reaction chamber, and a pumping system. The reaction chamber was evacuated to 1×10^{-4} Pa using a turbomolecular pump before irradiation by the SR beam.

Figure 1 (a) shows an experimental setup used for SR ablation. The PTFE, PE (polyethylene), $C_2H_2F_2$ thick films as a target were set perpendicularly to the SR beam in the reaction chamber. The sample heating was carried out using carbon heater. The sample temperature was monitored with a thermocouple in contact with the surface of sample. The SR ablation was carried out in vacuum.

On the other hands, figure 1 (b) shows experimental set up used for SR induced reaction. The substrate were set perpendicularly to the SR beam. The hydrocarbon and fluorocarbon gases were generated in the reaction chamber by evaporating PE and $C_2H_2F_2$ targets using carbon heater. The SR beam irradiated the target at 1×10^{-2} Pa.

RESULTS

Figure 2 shows a scanning electron microscopy (SEM) image of particles deposited on substrate using SR ablation of PTFE at dose of 1500 mA·min and a sample temperature of 500 °C. The size of particles were less than 1 μm.

Figure 3 shows a SEM image of particles deposited on the SR irradiation region on substrate using PE evaporation. The deposits with hemispherical shape of about 3 μm size were observed. In the case using $C_2H_2F_2$ evaporation, on the other hand, these deposits were not observed on the substraete.

Evaluation of deposits are being carried out using XPS and FT-IR. Moreover, emission characteristics will be investigated for the samples fabricated in this study.

REFERENCES

[1] M. Inayoshi *et al*, Jpn. J. Appl. Phys., **34**, L1675 (1995).

[2] M. Inayoshi *et al*, J. Vac. Sci. Technol., **B 17**, 949 (1999).

[3] H. Nagai *et al*, Applied Surface Science **183**, 284 (2001).

[4] H. Nagai *et al*, UVSOR Activity Report 182 (1999).

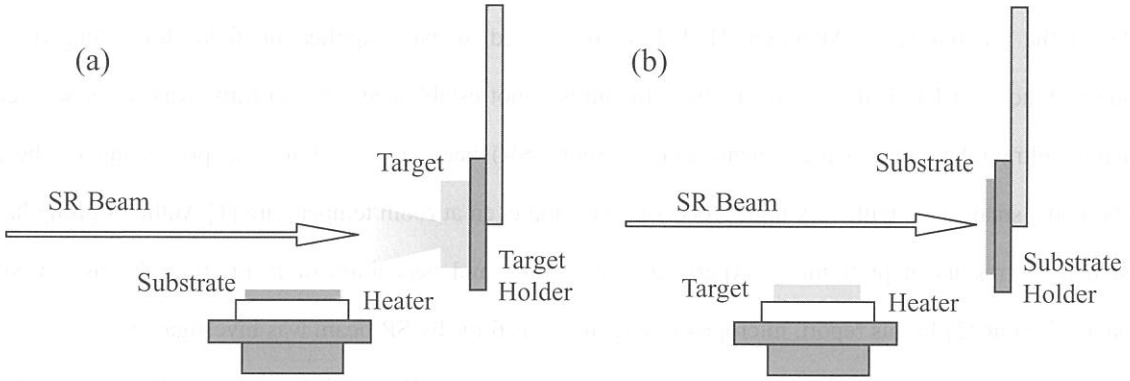

Fig. 1 Experimental set up used for (a) SR ablation and (b) SR induced reaction.

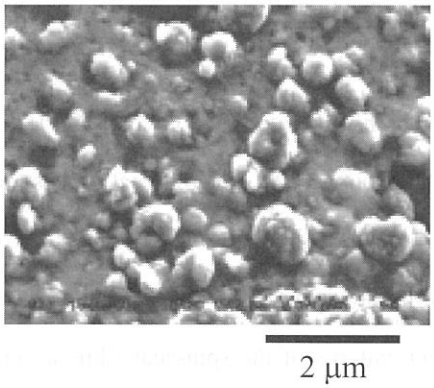

Fig. 2. SEM image of particles deposited on substrate using SR ablation of PTFE at substrate temperature of 500 °C.

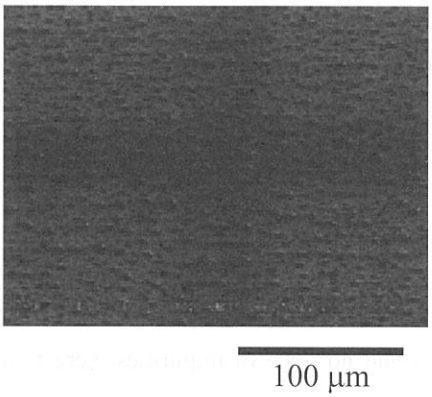

Fig. 3. SEM image of particles deposited on the SR irradiation region on substrate using PE evaporation.

(BL8A)

Formation of Polytetrafluoroethylene Microstructures by Synchrotron Radiation

H. Okada, E. Matsumoto, H. Yamada A. Wakahara and A. Yoshida

Department of Electrical and Electronic Engineering, Toyohashi University of Technology, Tempaku-cho, Toyohashi, 441-8580, Japan

Recent progress in micro-fabrication technique opens a new field of the microsystem such as the micro-machines, micro-sensors etc. Polytetrafluoroethylene (PTFE) is known to have unique properties: superior chemical stability, high thermal stability, high hydrophobicity and so on. These unique features of PTFE seems valuable for the microsystems. Although PTFE have been used in many application fields for a long time, formation technique of PTFE thin films or microstructures is not established yet. Recently, Kato *et al* showed that vacuum ultraviolet light in the synchrotron radiation (SR) beam is useful for the processing of these materials on the small scale with very high processing rate and even at room temperature.[1] Author's group has reported that the results of preliminary experiments of etching and deposition of PTFE films by use of SR radiation at UVSOR.[2] In this report, microprocessing of PTFE films by SR beam was investigated.

Experimental arrangement for a microprocessing is shown in Fig.1. The SR beam was incident through the same Ni mesh mask onto the spin-coated films. Thus, limited area ethicng of the PTFE film is expected here. Etching experiments were carried out in the reaction chamber having differential evacuation system was connected to the BL-8A port in UVSOR.

For the sample preparation, commercially available PTFE emulsion was used as a source of PTFE thin films. This source contains PTFE fine particles and surfactant. The rotational speed in the spin-coat process was 4000 rpm for 60sec, and the wafers were baked and filmed for 10min at the temperature of 513-673K. From x-ray photo-spectroscopy (XPS) spectrum of the deposited PTFE film shown in Fig.2, only C and F peaks were observed and no trace of impurities were found. From the XRD patterns of the spin-coat films a very strong sharp peak due to (100) plane of PTFE was observed. Thus, the crystalline quality of the films was obtained. The surface of the films was very smooth from atomic force microscope (AFM) observation, as shown in Fig.3.

The surface of PTFE is etched/ablated by irradiating SR beam and only irradiated surface region was easily etched through a mask. Nano-structured fabrication on the PTFE surface is possible with a suitably patterned mask. We tried the etching of commercially available PTFE sheet, and SR-induced and spin-coated PTFE thin

films through the Ni metal mask. The etching rate was very high (6mm/min for the electric current of 230mA in the storage ring), and was linearly dependent on the photon flux in proportion to the electron beam current in the storage ring. Figure 4 showed the SEM image of the etched surface of spin-coated PTFE films, and the PTFE surface was easily etched only on the area exposed to SR beam. By using SR-assisted process only, it is possible to deposit the crystalline PTFE films and succeedingly etch the surface of these films on a micro-scale. Since the SR beam is straightforwardly incident, the distance between a mask and the surface is allowed to be large even on a nano-structure. When the spin-coat method is accepted, the smooth and flat surface of PTFE is obtained even on complicated surface of the substrates.

REFERENCES
[1]T.Katoh and Y.Zhang, Appl.Phys.Lett., 68 (1996) 865
[2]M.Uchida, M.Ishizaka, H.Okada, A.Wakahara and A.Yoshida, UVSOR Activity Report 2000, (2000) 216

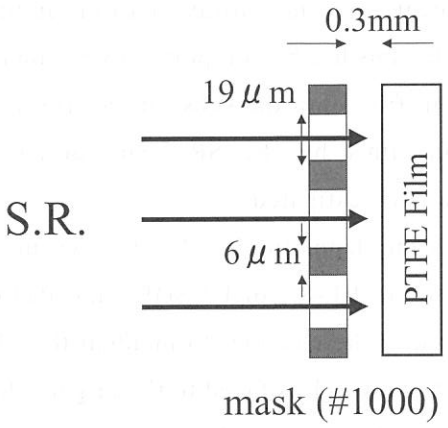

Fig.1: Experimental setup for etching.

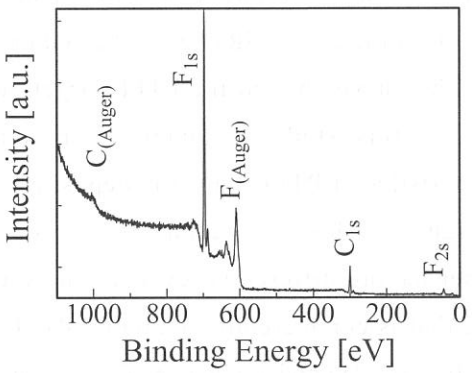

Fig.2: XPS spectrum of spin-coated PTFE film.

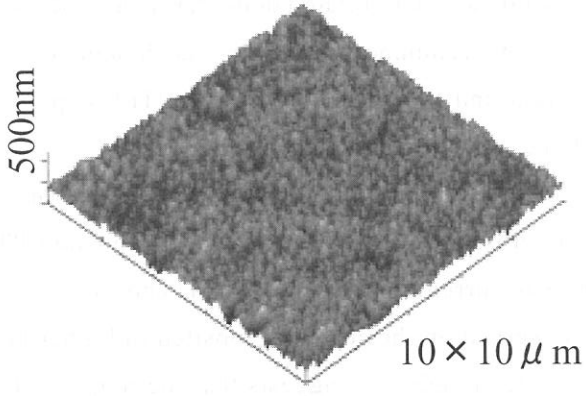

Fig.3: AFM image of spin-coated PTFE film.

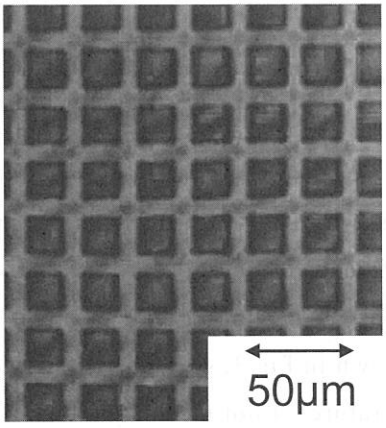

Fig.4: SEM image of etched film.

(BL8A)

Characteristics of Polytetrafluoroethylene Films Deposited by Synchrotron Radiation

A.Yoshida, E.Matsumoto, H.Yamada, H.Okada and A.Wakahara

Department of Electrical and Electronic Engineering, Toyohashi University of Technology, Tempaku-cho, Toyohashi, 441-8580, Japan

Polytetrafluoroethylene (PTFE) is a fascinating material due to its superior chemical stability, high thermal stability, high hydrophobicity and low surface tension. Adding to these, it also has excellent electrical characteristics, such as high breakdown voltage with low dielectric constant (ε_s=2.1). In spite of these features, formation or patterning of PTFE thin films are thought to be difficult due to the aforementioned nature. Recently, vacuum ultraviolet light in the synchrotron radiation (SR) beam utilized processing of PTFE films has been reported by Katoh *et al.*[1] They have ablated the PTFE target, and deposited thin film onto the substrate nearby the target. In this study, to obtain high quality PTFE thin films by the SR beam process, characteristics of PTFE thin film deposited by SR process was investigated.

Figure 1 shows experimental setup for PTFE thin film deposition[2, 3]. The vacuum chamber having differential evacuation system was connected to BL-8A of UVSOR ring. PTFE target, that is commercially available PTFE lump, was placed in the chamber to incident the SR beam directly. Deposition was made onto the p-Si(100) substrate which is faced to the target. The distance between the target and Si substrate was 3cm. Target heating can be achieved with a target heater.

Figure 2 showes Fourier transformation infrared (FTIR) spectrum of the PTFE thin film deposited at room temperature. Absorptions can be seen at the wavenumber of 1207、1152、630、553、 502cm^{-1}. Observed absorption peaks are assigned as CF_2 related bond that is a fundamental composition in PTFE. Weak peak observed at the wavenumber of 980cm^{-1} is thought to come from CF_3 bond. We have changed the beam current and target temperature in PTFE deposition, however, change was not observed in the FTIR spectrum from the deposited film.

Target temperature dependence of the surface morphology of the deposited film was investigated. Figure 3 shows the atomic force microscope (AFM) image of the deposited PTFE film for various target temperatures. Here, the beam current in storage ring was chosen at 220mA. As shown in Fig.3, granular-like structure was observed on the surface deposited in higher target temperatures. Root mean square (RMS) of the surface roughness suggests that the rough surfaces appear in higher target temperatures. Thus, target temperature affects the surface morphology.

As compared with the previous report in Ref.1, larger deposition rate was obtained in our results. From the sharpness of the XRD peak of the deposited film, the film deposited in this study seems to have good crystallinity. At present, fair comparison between two reports is

difficult, however, one possibility of the observed sharp XRD peak in this study is a utilization of focused SR beam in BL-8A. Indeed, the vacuum pressure of the chamber went up to 10^{-4}Torr during the deposition process. In such a situation, enhanced reaction is expected due to the existence of large amount of saturated fluorocarbon species in between the target and. This may lead to cause a high crystal PTFE film depostion.

REFERENCE
[1] T.Katoh, Y.Zhang, Appl. Phys. Lett. 68, 6 (1996) 865.
[2] M.Uchida, M.Ishizaka, H.Okada, A.Wakahara and A.Yoshida, UVSOR Activity Report 2000,(2000) 216.
[3] E.Matsumoto, M.Uchida, H.Okada, A.Wakahara and A.Yoshida, Technical Report of IEICE, SDM2001-30~43 (2001) 7.

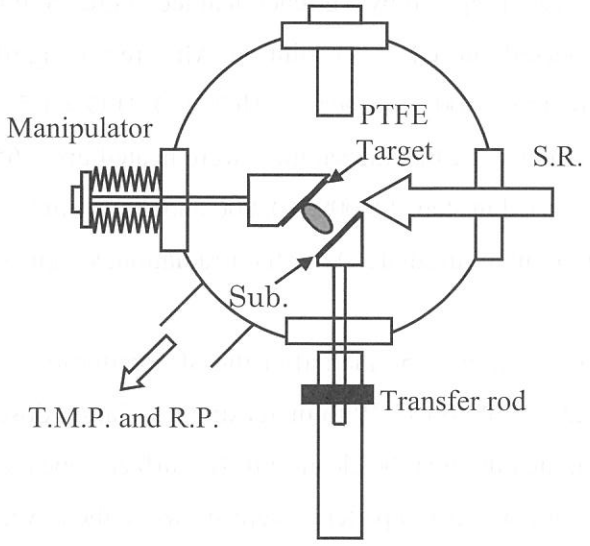

Fig.1 Experimental setup

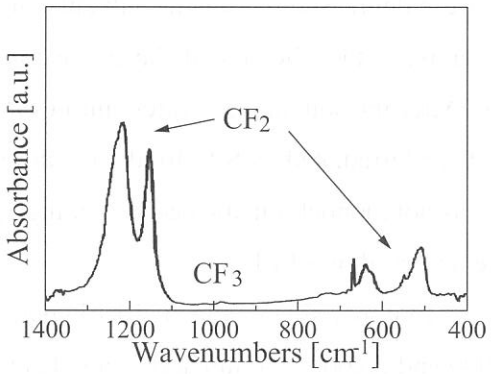

Fig.2 FTIR spectrum of PTFE thin film

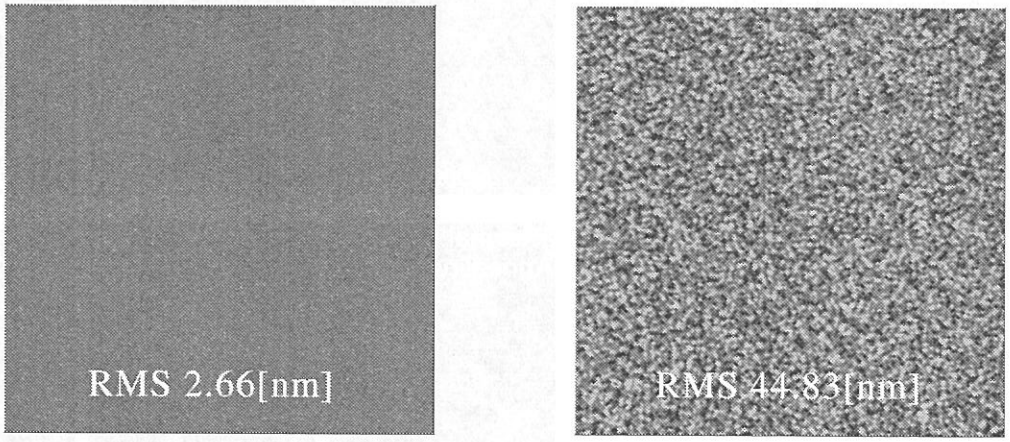

(a) Target Temperature R.T. (b) Target Temperature 210℃

Fig.3 AFM images of PTFE thin film($10\times10\,\mu$m)

(BL6B)

Silicon Oxide on Si (001) Surfaces Removed by SR Stimulated Desorption

Youichi NONOGAKI and Tsuneo URISU

Institute for Molecular Science, Myodaiji, Okazaki 444-8585, Japan

By SR irradiation to the solid surfaces, various kinds of surface photochemical reactions occur due to strong interaction between VUV light and materials. So far, we have investigated SR stimulate silicon oxide desorption reaction on Si (111) surfaces by scanning tunneling microscope (STM) and low energy electron diffraction (LEED). From the STM observations, we have observed significant difference on the surface structures between usual thermal desorption and SR stimulated desorption on Si (111) surface. In this report, silicon oxide SR stimulated desorption on Si (001) by LEED observation.

Si (001) wafers covered by silicon oxide were prepared by wet-chemical technique. Si (001) wafers were degreased by organic solvents and immersed into HF (5%) solution. After removing of native silicon oxide, the silicon oxide layer was formed on the Si (001) surfaces by $HCl:H_2O_2:H_2O$ = 1:5:10 solution. After introducing the wafers into UHV chamber at BL6B, the samples were heated up to 650°C or 700°C and irradiated by SR. Irradiation dose was varied in step at 5,000, 10, 000 and 20,000 mA min. The SR was not monochromatic because of high photon flux to irradiate. After the irradiation, sample surfaces were observed by LEED.

In upper side of Fig. 1, LEED patterns were shown obtained after the SR irradiation of 5,000, 10,000 and 20,000 mA min at the sample temperatures of 700°C. With increasing irradiation dose, 2 x 1 pattern appears and the each spot becomes clear, indicating that the clean Si (001) surface appears and the area of clean surface increases gradually. For comparison, LEED patterns were shown in the lower side of Fig. 1 obtained after thermal annealing at the same temperature of 700°C without SR irradiation. The annealing times were set at 22, 49, 90 min, which corresponds to the duration time for 5,000, 10,000 and 20,000mA min irradiation of upper side samples. All the LEED images have no spots, indicating that surface oxide remains even for 90 min annealing.

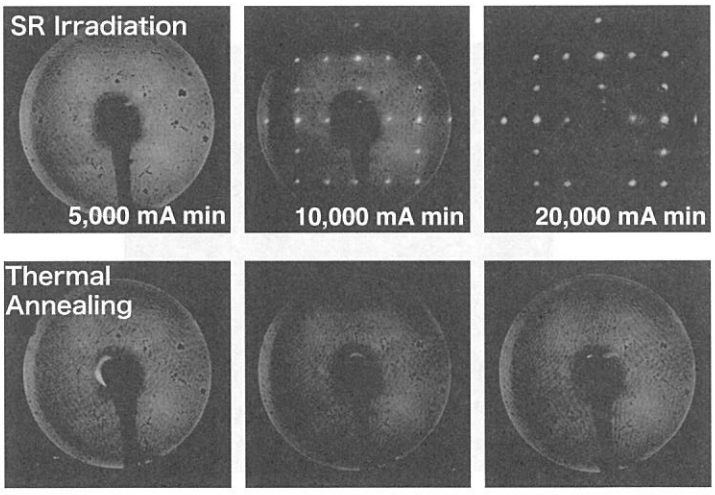

Figure 1: LEED patterns after SR irradiation at 700°C in upper side. In the lower side, LEED patterns after thermal annealing without SR irradiation

This result means that silicon oxide on Si (001) is removed by SR stimulation effect. This phenomenon can be applied to make silicon oxide patterns on Si (001) surfaces by the area selective desorption using SR irradiation.